# Characterization of Silicon-Stabilized Amorphous Hydrogenated Carbon

*W.C. Vassell, A.K. Gangopadhyay, T.J. Potter, M.A. Tamor, and M.J. Rokosz*

**The characterization of a modified form of diamondlike carbon, referred to as silicon-stabilized amorphous hydrogenated carbon (Si-AHC), is described. Auger electron spectroscopy, electron probe microanalysis, solid-state nuclear magnetic resonance, Raman scattering, nuclear reaction analysis, and optical absorption spectroscopy were used to determine chemical composition and to monitor structural changes due to the addition of silicon. Hardness, density, residual stress, and tribological properties of AHC and Si-AHC are compared. The Si-AHC coatings show much lower stress, a friction coefficient that is insensitive to moisture, an increase in optical gap compared to AHC, improved thermal stability, and equivalent hardness and wear. Some automotive applications are discussed.**

**Keywords** amorphous carbon coatings, atomic structure, automotive applications, tribology

## 1. Introduction

Despite properties that make diamondlike carbon (DLC) films ideally suited as protective coatings, there has been no reported commercial use of this material in high-stress tribological applications (Ref 1). Diamondlike carbon has become an umbrella term that is used to refer to a broad range of carbon-base materials generally deposited as amorphous films. While DLC materials often exhibit some medium-range ordering in the form of graphitic planar rings, there has been no direct evidence for the existence of the cubic diamond phase, and only indirect evidence for microcrystalline hexagonal diamond (Ref 2). Although deposition techniques for DLC are relatively straightforward compared to the experimental procedures necessary for diamond film deposition, characterization of DLC films is considerably more difficult because of their more complex bonding arrangements (Ref 3, 4). In general, DLC materials are hard (10 to 20 GPa), chemically inert, have low friction surfaces (coefficient < 0.1 against steel) and low wear, and can be deposited at low temperatures (<100 °C) and pressures (1 to 20 Pa). In this paper, amorphous carbon that contains hydrogen will be referred to as amorphous hydrogenated carbon (AHC).

A variety of analytical techniques were used to study the chemical and structural nature of the various forms of AHC at the atomic level, including Auger electron spectroscopy (AES), electron probe microanalysis (EPMA), optical absorption, nuclear magnetic resonance (NMR), nuclear reaction analysis, and Raman scattering. In addition, measurements of mechanical and tribological properties such as hardness, density, stress, friction, and wear were performed to better understand the possible use of AHC films in automotive applications, where reduction of friction and wear would have a major impact on increasing durability, reliability, safety, and on reducing warranty costs.

The general properties of DLC materials would seem ideal for a coating for use in surface engineering. However, various issues have limited their use in industrial applications. As deposited, the films are under high compressive stress, which limits their thickness to less than about 2 μm (Ref 5). They show a marked increase in friction with increasing relative humidity (Ref 6, 7). Also, at temperatures above about 300 °C, hydrogen begins to evolve from hydrogenated films and the structure becomes more graphitic, with a resulting decrease in hardness and an increase in friction and wear. Finally, coatings deposited directly onto ferrous substrates show poor adhesion. Modifications of the DLC structure to reduce or eliminate these effects have been reported, and several reviews discuss these problems along with a general description of the present understanding of both the experimental and theoretical aspects of amorphous carbon films (Ref 8-12).

This paper discusses the modification of AHC by incorporation of silicon into the carbon structure and reports on measurements directed toward characterization of the resulting material, referred to as silicon-stabilized AHC (Si-AHC). Addition of silicon to AHC was first reported by Oguri and Arai (Ref 13, 14), who used toxic precursor gases at relatively high temperatures (550 °C) to introduce silicon into their films. However, present safety and environmental concerns discourage the use of such chemicals in large-scale industrial applications.

## 2. Experimental

The films were deposited in a radio-frequency (RF) plasma formed from hydrocarbon gases appropriate for deposition of the carbon and for the introduction of silicon into the structure. Films to be used for analysis were deposited in a capacitively coupled self-biased parallel plate reactor with substrates placed on the negative electrode. A variety of substrate materials were used, including silicon, aluminum, steel, and quartz. Automotive components were either aluminum or steel and were coated in a larger chamber by applying the RF power directly to the part. This produces a uniform coating even on complex three-dimensional shapes and is better described as conformal-plasma reactive ion plating (CP-RIP) than as plasma-enhanced chemical vapor deposition (PE-CVD) (Ref 15). In both cases, ions from the plasma are accelerated toward the substrate by the bias potential.

**W.C. Vassell, A.K. Gangopadhyay, T.J. Potter, M.A. Tamor,** and **M.J. Rokosz,** Ford Motor Research Laboratory, Dearborn, MI 48121-2053, USA.

Substrates could be biased from 0 to −1300 V with power densities ranging from 0.2 to 0.6 W/cm$^2$. Flow rates of all precursor gases were adjusted separately with mass flow controllers so that the silicon content of the films could be controlled. Coatings were deposited directly onto the substrates surfaces except for the steel samples, where an interlayer film was required for good adhesion. Aluminum, silicon, titanium, tungsten, or chromium films can be used as interlayers. Film thickness ranged from about 0.02 μm to more than 10 μm at deposition rates ranging from 1.5 to 3 μm/h.

Hardness measurements were made with an ultra-microindenter, using a 5 μm spherical diamond tip. The residual stress in the coating was determined by measuring the deflection of a coated rectangular strip with a profilometer and calculating the stress from:

$$\sigma = \frac{4E_s t_s^2 \delta}{3(1-\nu)L^2 t_f} \quad \text{(Eq 1)}$$

where $E_s$ is Young's modulus of the substrate, $t_s$ is the substrate thickness, $\delta$ is the deflection, $\nu$ is Poisson's ratio, $L$ is the deflection scan length, and $t_f$ is the film thickness (Ref 16, 17).

## 3. Characterization

### 3.1 *Chemical and Structural*

Auger electron spectroscopy was used initially for quantitative chemical analysis of the coatings. A depth profile was obtained by alternately scanning the surface, removing material by argon ion sputtering, and then repeating the process until the substrate was exposed. Measurements by EPMA were initiated for comparative purposes. This technique samples a larger volume of material than AES and is less sensitive to structural variation. Vitreous carbon and crystalline silicon were used as standards because their x-ray line shapes were a close match to those of the samples. Results of the two methods are compared in Fig. 1.

Carbon-to-silicon ratios in the film as a function of the same ratios in the precursor gases are shown in Fig. 1(a). Although the disparity in absolute value is large, the curves track with a systematic difference of approximately 4, most likely due to an incorrect choice of reference material for the AES analysis. The microprobe results for silicon content are used based on their closer correlation with the silicon content in the vapor, as can be seen in Fig. 1(a).

Subsequent determination of the hydrogen concentration by nuclear reaction analysis using $^{15}N$ as the probe beam established that the hydrogen concentration remained essentially constant (30 to 32 at.%), while the silicon content ranged from 5 to 23 at.%. For films containing no silicon, the hydrogen concentration was measured at 28 at.%. Important information for process control is shown in Fig. 1(b), where the percent of silicon in the film including hydrogen is plotted as a function of the silicon in the vapor.

### 3.2 *Raman Spectroscopy*

Raman scattering has proved to be an important analytical technique in characterizing both diamond and AHC films. The sharp 1332 cm$^{-1}$ line due to C-C stretch vibrations is direct evidence of the presence of crystalline diamond. Raman spectra of AHC are less definitive and are characterized by broad bands centered at approximately 1550 cm$^{-1}$ (G-peak) and 1350 cm$^{-1}$ (D-peak), which vary in width, position, and intensity depending on deposition parameters (Ref 18-21). A detailed analysis of Raman spectra of DLC films relating spectral and line-shape variations to film properties has recently been reported (Ref 22). Besides the G and D bands, the spectra of Si-AHC films also showed a small broad band at 800 cm$^{-1}$, which appeared only in AHC containing silicon (Fig. 2b). Optical phonons of silicon carbide (SiC) lie in this region and have been shown to broaden in disordered and in carbon-rich material (Ref 23-25). The phonon positions for crystalline silicon and silicon carbide are labeled Si and SiC, respectively, in Fig. 2(b).

The Raman spectrum in Fig. 2(b) shows evidence not only of amorphous SiC but also of silicon clustering as indicated by the band at about 500 cm$^{-1}$, which is characteristic of amorphous silicon and which is not apparent in films with silicon content below about 20 at.%.

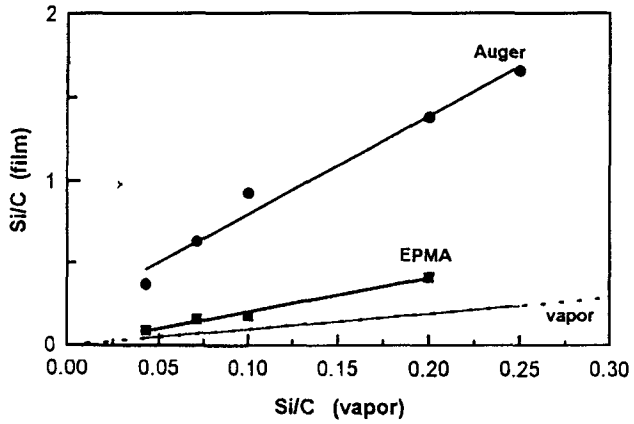


(a)

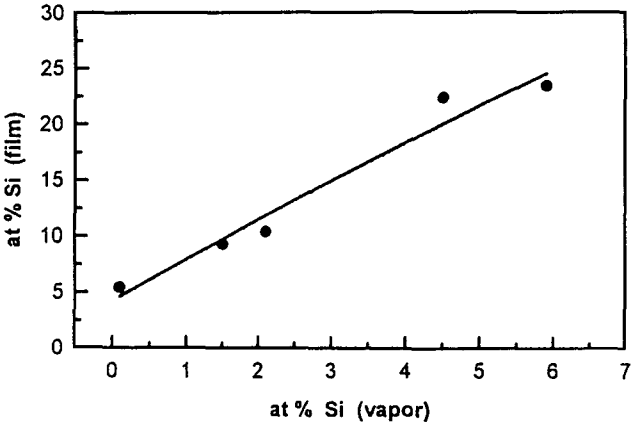


(b)

**Fig. 1** (a) The Si/C ratio in the films as a function of Si/C ratio in the vapor. (b) Atomic percentage of silicon as determined by EPMA. Hydrogen was included in the determination. Films were deposited at −500 V bias.

### 3.3 *Optical Absorption*

Optical absorption in AHC has been shown to be due to electronic transitions between $\pi$ bond states within the $sp^2$ graphitic clusters that form part of the overall matrix (Ref 20, 21). The behavior of the optical gap, $E_g$, as a function of bias voltage used during deposition is shown in Fig. 3. The value of $E_g$ for the films was determined by fitting absorption data to the Tauc equation:

$$\alpha E = B(E - E_g)^2 \quad \text{(Eq 2)}$$

**Table 1 Coordination fraction for protonated and unprotonated $sp^2$ and for total $sp^3$ as determined by NMR**

| | AHC | | | | Si-AHC | | | |
|---|---|---|---|---|---|---|---|---|
| Bias, V | $sp^2_C$ | $sp^2_H$ | $sp^2_{total}$ | $sp^3_{total}$ | $sp^2_C$ | $sp^2_H$ | $sp^2_{total}$ | $sp^3_{total}$ |
| -250 | 0.3 | 0.11 | 0.43 | 0.59 | 0.27 | 0.15 | 0.42 | 0.58 |
| -500 | 0.37 | 0.26 | 0.63 | 0.37 | 0.32 | 0.17 | 0.49 | 0.52 |
| -750 | 0.45 | 0.25 | 0.70 | 0.30 | ... | ... | ... | ... |
| -1000 | 0.54 | 0.24 | 0.78 | 0.22 | ... | ... | ... | ... |
| -900 | ... | ... | ... | ... | 0.34 | 0.21 | 0.55 | 0.44 |

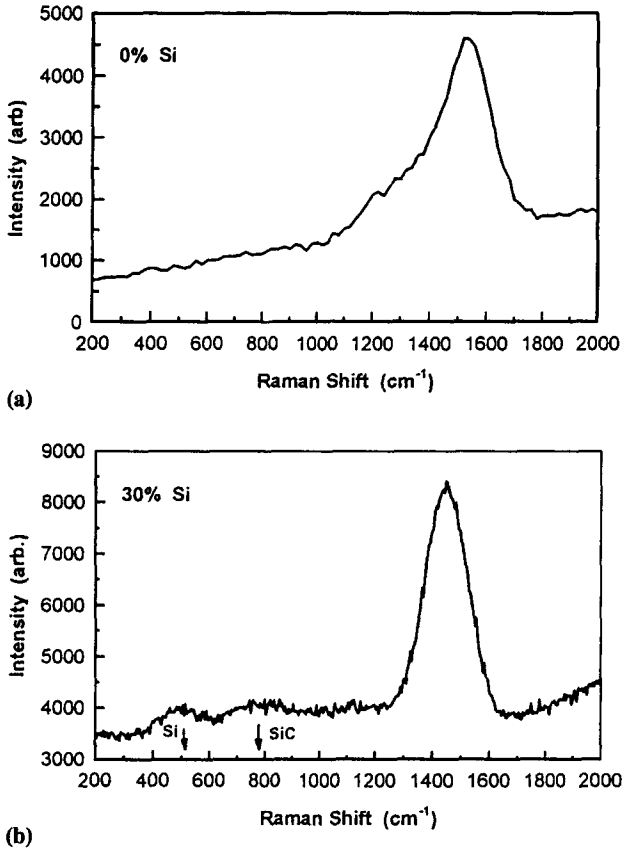


**Fig. 2** Raman spectra of AHC (a) and Si-AHC (b). The band at about 800 $cm^{-1}$ was evident in films containing even a few percent silicon, while the band at 500 $cm^{-1}$ was evident only in those with more than about 20 at.%. Films were deposited at -500 V bias.

where $\alpha$ is the absorption coefficient, $E$ is the photon energy, and B is a parameter determined by the material and is the same for all the films (Ref 26). Originally derived by Tauc et al. (Ref 26) to describe transitions between parabolic bands in crystalline semiconductors, it was later shown by Mott and Davis (Ref 27) to apply to optical absorption in amorphous materials as well. The generally larger values of $E_g$ in Si-AHC indicate that silicon is effective in reducing both the number and size of graphitic clusters, thereby reducing the $\pi$ bonding that is responsible for the much smaller optical gap of AHC compared to diamond. From the slopes of the plots in Fig. 3(a), one obtains a 56% decrease in $E_g$ for AHC as compared to a 20% decrease for Si-AHC over the same bias range. A recent analysis of the effects of disorder on cluster size, formation of different types of $sp^2$ sites (rings or chains), and optical gap is given by Robertson (Ref 28).

### 3.4 *Nuclear Magnetic Resonance*

The effect of silicon on stabilizing against $sp^2$ formation was further demonstrated by NMR measurements of the carbon coordination in Si-AHC. Measurements were made using solid-state magic angle spinning on $^{13}C$, with the natural abundance of this isotope normally present in carbon providing sufficient signal. Experimental details are given in previous studies with unmodified AHC (Ref 29, 30).

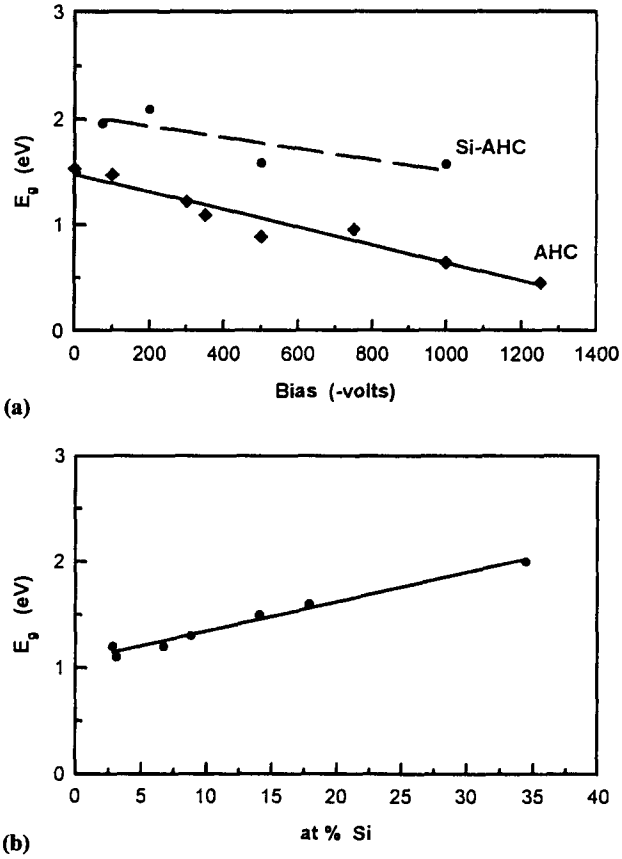


**Fig. 3** Variation of band gap with bias (a) and with silicon content (b). Silicon concentration of films in (a) was about 25 at.%. All the films in (b) were deposited at the same bias.

Table 1 compares the results for AHC with the recent work on Si-AHC. The designations $sp^2_C$ and $sp^2_H$ refer to unprotonated and protonated $sp^2$ bonding, respectively. The stabilizing effect of silicon is clearly demonstrated by comparing the 80% increase of the total $sp^2$ bonds for AHC with the 30% increase for Si-AHC as the bias is increased. This correlates with the results obtained from the optical measurements discussed earlier. Similarly, the *decrease* of $sp^3$ bonds with increasing bias was *reduced* from 63% for AHC to 24% for Si-AHC. Quantitative analysis of the silicon coordination in these measurements has proved to be more complex and will be reported in the future. However, there are preliminary indications of a sharp increase in Si-Si bonding at high bias (~900 V).

### 3.5 *Mechanical and Tribological*

Tribological characterization of hard films is of prime importance in determining the suitability of any particular film material for a specific engineering application. Ultimately, the two most important parameters in tribology are friction and wear. These, however, are strongly influenced by mechanical properties such as hardness, density, and residual stress. A large compressive stress has been the single most important factor limiting the use of unmodified DLC in tribological applications because of the limit it places on coating thickness (<2 μm) and its adverse effect on adhesion.

A comparison of these properties for AHC and Si-AHC is shown in Fig. 4 to 6. Figure 4 shows that silicon provides a large decrease in stress and an expected increase in density due to substitution of carbon by heavier silicon. The hardness is virtually unaffected by the addition of silicon, while the moisture sensitivity of the friction coefficient is eliminated, as shown in Fig. 5. Detailed tribological studies of AHC films were reported previously (Ref 7, 31, 32). Here some of those results are compared with measurements of Si-AHC. Friction coefficient and film wear are shown in Fig. 6. The AHC films in Fig. 5 and 6 were deposited under the same conditions as the Si-AHC films. Table 2 compares the wear of AHC and Si-AHC with other hard coatings.

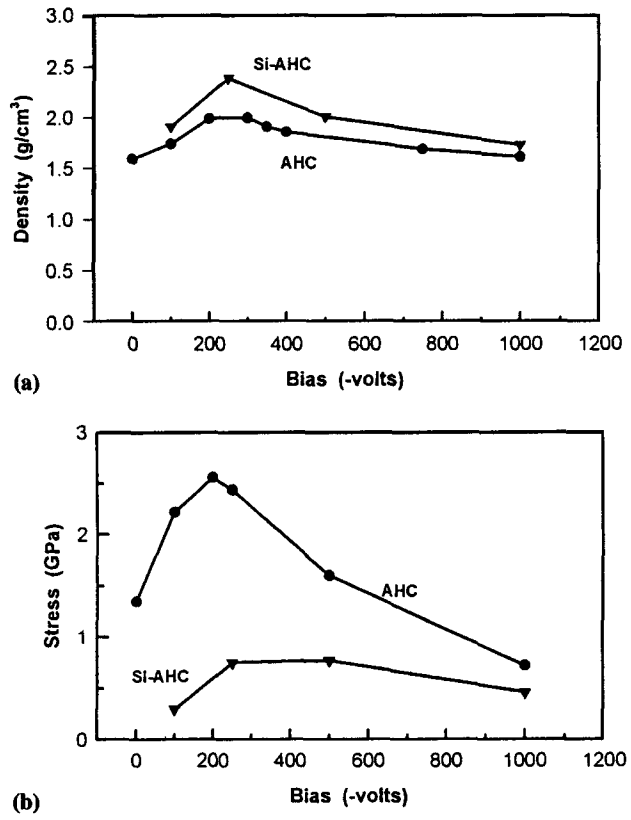


**Fig. 4** Effect of silicon on density (a) and residual stress (b). The Si-AHC films in both cases contained about 10 at.% Si.

**Table 2 AHC and Si-AHC compared to other hard coatings(a)**

| Test load, N | Disk coating(b) | Ball wear, $mm^2/N \cdot m$ | Coating wear, $mm^2/N \cdot m$ | Ref |
|---|---|---|---|---|
| 10 | PVD Ti(BN) | $7 \times 10^{-7}$ | $1.1 \times 10^{-5}$ | 33 |
| 2.5 | CVD TiN | $10^{-5}$ | $10^{-5}$ | 34 |
| 4 | CVD TiC | $2.55 \times 10^{-6}$ | | 35 |
| | CVD TiN | $1.53 \times 10^{-5}$ | | |
| 4.2 | AHC | $1.5 \times 10^{-8}$ | $1.5 \times 10^{-6}$ | (c) |
| 4.2 | Si-AHC | $1.7 \times 10^{-7}$ | $1.9 \times 10^{-7}$ | (c) |

(a) Contact geometry, steel ball on disk. (b) PVD, physical vapor deposited; CVD, chemical vapor deposited. (c) Author data

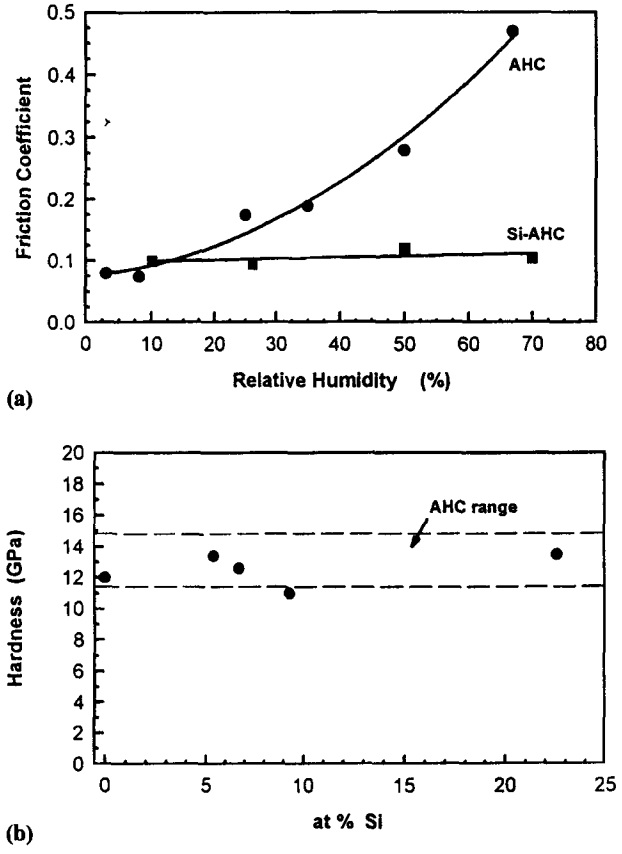


**Fig. 5** (a) Friction coefficient as a function of relative humidity for unlubricated sliding. Measurements were made by ball on disk. (b) Comparison of hardness of Si-AHC with that of AHC. The dashed lines indicate the range of values for AHC films.

### 3.6 *Thermal Effects*

Depending on the specific application, protective coatings applied to automotive components could encounter temperatures exceeding 800 °C. It is important, therefore, that the thermal stability of coatings considered for use in an automotive environment be investigated. In general, AHC is unstable in vacuum at temperatures above approximately 300 °C,where hydrogen begins to evolve and the film gradually becomes graphitic (Ref 36). Studies of AHC films heated in vacuum have shown that the friction coefficients of films were comparable to as-deposited films for temperatures up to about 400 °C, but showed poor wear when heated to higher temperatures (Ref 37). Since automotive components operate largely in air, it is important that the friction and wear properties of coatings at elevated temperatures in air be known.

Figure 7(a) shows the weight loss per unit surface area for an uncoated silicon wafer, an AHC film, and a Si-AHC film, all heated in air for 2.5 h at each temperature. Measurements could be made on AHC films up to 450 °C, at which point the film was completely consumed, while the temperature for complete film consumption for Si-AHC films was about 650 °C. Also, the onset of weight loss is shifted upward by almost 100 °C by the addition of silicon. These results indicate a greater resistance to oxidation of Si-AHC. Furthermore, the Raman spectra in Fig. 7(b) of these films showed diamondlike characteristics until the temperature exceeded 488 °C (approximately the same temperature as the onset of weight loss due to oxidation), at which point the spectra indicated increased graphitization.

To test the thermal stability in the absence of oxygen, Si-AHC films on silicon substrates heated to 670 °C under flowing argon gas showed no visible changes. The Raman spectra were altered slightly toward graphite, but remained within the range associated with diamondlike properties. Tests showed that the friction and wear were comparable to as-grown films. However, the large compressive stress always present in AHC was reduced and even became tensile in some instances. This suggests that, despite some hydrogen evolution and an increase in graphitic component during heating, the presence of silicon stabilizes the network against total thermal decomposition. This extended thermal stability of Si-AHC makes it more suitable for higher-temperature engine applications and implies that a hard, lower-stress film could be deposited at elevated temperatures.

## 4. Applications

Tests of automotive components coated with Si-AHC have ranged from the use of the coating as a corrosion barrier to its use as a wear-resistant tribological coating in high-stress pow-

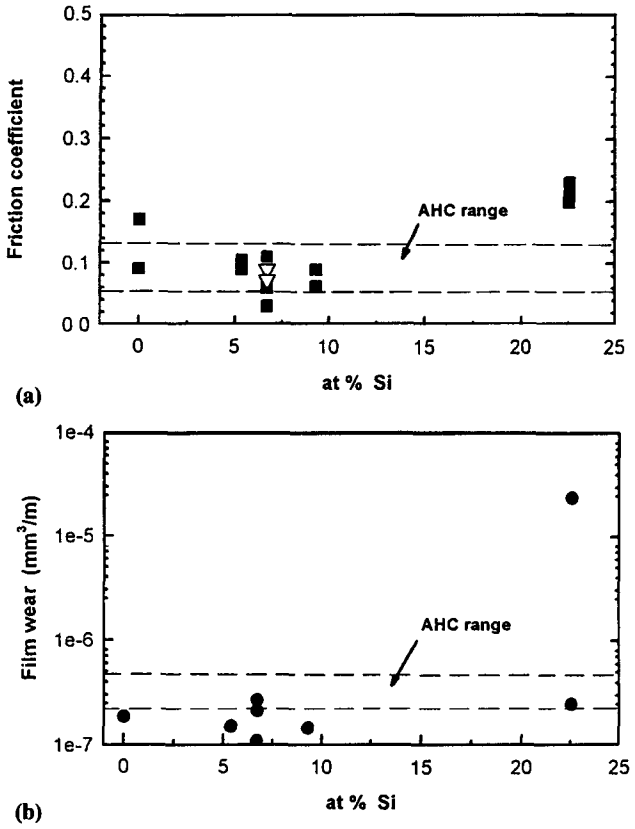


**Fig. 6** Friction and wear of Si-AHC films as a function of silicon content as determined by ball-on-disk measurements with films on silicon substrates. The dashed lines indicate the range of values for AHC films under similar conditions.

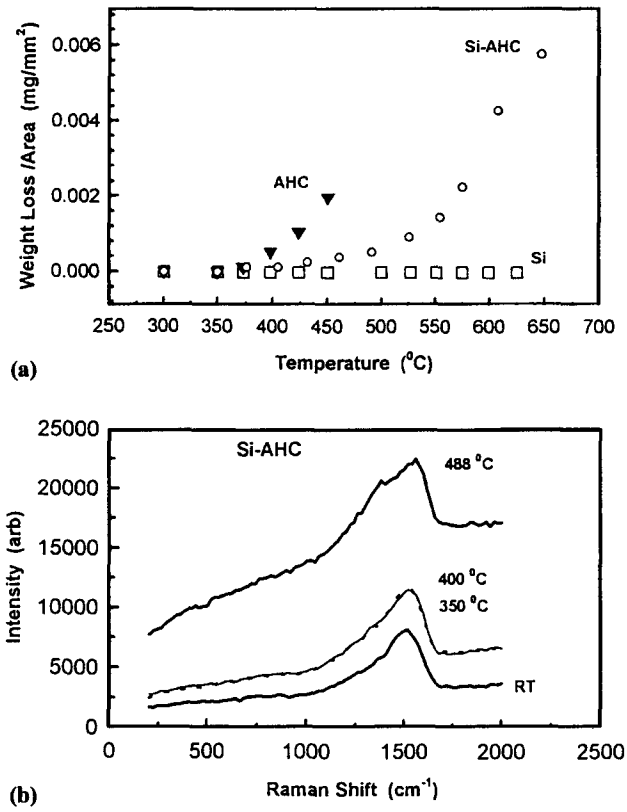


**Fig. 7** (a) Weight loss (2.5 h exposure to air) for AHC and Si-AHC as a function of annealing temperature. (b) Raman spectrum of Si-AHC samples taken after annealing at three different temperatures.

ertrain applications, including the engine. Thermal environments have ranged from outside ambient air to internal engine temperatures. A dramatic example of the protection against mechanical failure that an approximately 3 μm Si-AHC film can provide is shown in Fig. 8. The transmission gear on the right was damaged by a test used to provide durability data under severe load conditions not normally encountered. On the left is a gear coated with Si-AHC that underwent the same test. The procedure involved running the transmission continuously for several hours at maximum torque in second gear and then for several hours in first gear. The damaged gear was unable to run the full test, while the coated gear completed the full test with no apparent damage to the gear or to the film. Also shown is a coated forming tap used in a manufacturing operation after having operated 20 times longer than the average life of uncoated taps. The tap was undamaged, and the coating showed essentially no wear. Other tests, still in progress, indicate that Si-AHC coatings may be able to withstand even higher peak temperatures during thermal cycling than the maximum steady-state temperatures reached in the laboratory.

## 5. Summary

Amorphous hydrogenated carbon films modified by the addition of silicon into the carbon structure show much lower stress than the unmodified material, a friction coefficient that is insensitive to moisture, an increased optical band gap, and increased thermal stability. At the same time, Si-AHC films maintain the high hardness, low friction and wear, and corrosion resistance characteristic of AHC coatings, while allowing greater film thickness.

Several analytical techniques were used to determine the properties that are believed to be important to the survival of a hard coating in engineering applications. These do not always provide a definitive answer as to the durability of a coating in a given application. The final determination must often be made under actual operating conditions—on the car or in the plant in the case of automotive applications. Predictability could be improved by a better understanding at the atomic and molecular levels of the reasons for component failures in severe tribological applications (e.g., high stress, high temperature).

Other methods for characterization of hard coatings are also being applied or developed, such as contact angle measurements for the determination of surface free energy as reported by Grischke et al. (Ref 38), which could prove to be important in the development of hard coatings with specific lubricating properties, and new erosive and abrasive wear tests for use in quality assurance recently discussed by Hutchings (Ref 39). Conceivably, an appropriate protective coating could be applied to most components of an automobile with some benefit, ranging from decorative to protection against failure of the most critical components.

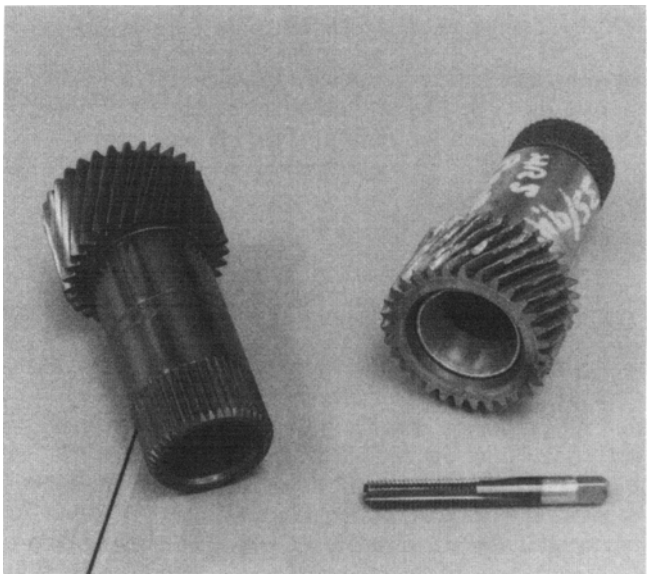

**Fig. 8** Transmission gear coated with Si-AHC (left) and uncoated gear (right), both subjected to severe load test. The uncoated gear suffered damage. At bottom is a coated forming tap. See text for details.


### Acknowledgments

We thank J.-S. Park and D.R. Liu for conducting the EPMA studies. The nuclear reaction analysis for hydrogen concentration was performed by Dr. H. Bakhru of Materials Diagnostics and the State University of New York at Albany.


### References


1. C. Donnet, Tribology of Solid Lubricant Coatings, *Condensed Matter News,* Vol 4 (No. 6), 1995, p 9
2. S.R.P. Silva, G.A.J. Amaratunga, E.K.H. Salje, and K.H. Knowles, Evidence of Hexagonal Diamond in Plasma-Deposited Carbon Films, *J. Mater. Sci.,* Vol 29, 1994, p 4962
3. J.E. Angus, Empirical Categorization and Naming of "Diamondlike" Carbon Films, *Thin Solid Films,* Vol 142, 1986, p 145
4. J. Robertson, Electronic Structure and Bonding of a-C:H, *Mater. Sci. Forum,* Vol 52-53, 1989
5. J.E. Angus and C.C. Hayman, Low-Pressure, Metastable Growth of Diamond and Diamondlike Phases, *Science,* Vol 241, 1988, p 913
6. K. Enke, H. Dimigen, and H. Hubsch, Frictional Properties of Diamondlike Carbon Layers, *Appl. Phys. Lett.,* Vol 36 (No. 4), 1980, p 29
7. A.K. Gangopadhyay, W.C. Vassell, M.A. Tamor, and P.A. Willermet, Tribological Behavior of Amorphous Hydrogenated Carbon Films on Silicon, *J. Tribol.,* Vol 116, 1994, p 454
8. J.E. Angus, P. Koidl, and S. Domitz, Carbon Thin Films, *Plasma Deposited Thin Films,* Vol 89, J. Mort and F.J. Jansen, Ed., CRC Press, 1986
9. J. Robertson, Amorphous Carbon, *Adv. Phys.,* Vol 35 (No. 4), 1986, p 317
10. J. Robertson, Properties of Diamondlike Carbon, *Surf. Coat. Technol.,* Vol 50, 1992, p 185
11. C.A. Davis, A Simple Model for the Formation of Compressive Stress in Thin Films by Ion Bombardment, *Thin Solid Films,* Vol 226, 1993, p 30
12. M.W. Geis and M.A. Tamor, Diamond and Diamondlike Carbon, *Encyclopedia of Applied Physics,* Vol 5, G.L. Trigg, Ed., VCH, 1993, p 1

13. K. Oguri and T. Arai, Low Friction Coatings of Diamondlike Carbon with Silicon Prepared by Plasma-Assisted Chemical Vapor Deposition, *J. Mater. Res.*, Vol 5 (No. 11), 1990, p 2567
14. K. Oguri and T. Arai, Tribological Properties and Characterization of Diamondlike Carbon Coatings with Silicon Prepared by Plasma-Assisted Chemical Vapor Deposition, *Surf. Coat. Technol.*, Vol 47, 1991, p 710
15. M.A. Tamor, Synthesis, Properties, and Applications of Superhard Amorphous Coatings, *Proc. 3rd Int. Conf. Application of Diamond Films and Materials,* National Institute of Standards and Technology, 1995, p 691
16. A. Brenner and S. Senderoff, Calculation of Stress in Electro-Deposits from the Curvature of a Plated Strip, *J. Res. Natl. Bur. Stand.*, Vol 4, 1949, p 105
17. B. Goranchev, K. Reichelt, J. Chevallier, P. Hornshoj, H. Dimigen, and H. Hubsch, R.F. Reactive Sputter Deposition of Hydrogenated Amorphous Siliconcarbide Films, *Thin Solid Films,* Vol 139, 1986, p 275
18. F. Tuinstra and J.L. Koenig, Raman Spectrum of Graphite, *J. Chem. Phys.*, Vol 53, 1970, p 1126
19. R.J. Nemanich, J.T. Glass, G. Lucovsky, and R.E. Shroder, Raman Scattering Characterization of Carbon Bonding in Diamond and Diamondlike Thin Films, *J. Vac. Sci. Technol.*, Vol A6 (No. 3), 1988
20. M. Ramsteiner and J. Wagner, Resonant Raman Scattering of Hydrogenated Amorphous Carbon: Evidence for $\pi$-Bonded Carbon Clusters, *Appl. Phys. Lett.*, Vol 5, 1987, p 1355
21. M. Yoshikawa, G. Katagiri, H. Ishida, and A. Ishitani, Raman Spectra of Diamondlike Amorphous Carbon Films, *J. Appl. Phys.*, Vol 64 (No. 11), 1988, p 6464
22. M.A. Tamor and W.C. Vassell, Raman "Fingerprinting" of Amorphous Carbon Films, *J. Appl. Phys.*, Vol 76 (No. 6), 1994, p 3823
23. P.V. Huong, Structural Studies of Diamond Films and Ultrahard Materials by Raman and Micro-Raman Spectroscopies, *Diamond Rel. Mater.*, Vol 1, 1991, p 33
24. L. Rimai, R. Ager, E.M. Logothetis, W.H. Weber, and J. Hangas, Preparation of Oriented Silicon Carbide Films by Laser Ablation of Ceramic Silicon Carbide Targets, *Appl. Phys. Lett.*, Vol 59 (No. 18), 1991, p 2266
25. N. Laidani, R. Capelletti, M. Elena, L. Guzman, G. Mariotto, A. Miotello, and P.M. Ossi, Spectroscopic Characterization of Thermally Treated Carbon-Rich $Si_{1-x}C_x$ Films, *Thin Solid Films,* Vol 233, 1993, p 114
26. J. Tauc, R. Grigorovici, and A. Yancu, *Phys. Stat. Sol.*, Vol 15, 1966, p 627
27. N.F. Mott and E.A. Davis, *Electronic Processes in Non-Crystalline Materials,* Clarendon Press, Oxford, 1971
28. J. Robertson, Structural Model of a-C and a-C:H, *Diamond Rel. Mater.*, Vol 4, 1995, p 297
29. M.A. Tamor, W.C. Vassell, and K.R. Carduner, Atomic Constraint in Hydrogenated Diamondlike Carbon, *Appl. Phys. Lett.*, Vol 58 (No. 6), 1991, p 592
30. K.R. Carduner, M.J. Rokosz, M.A. Tamor, and W.C. Vassell, Solid-State NMR Study of Carbon Bonding in Amorphous Hydrogenated Carbon Films, *Appl. Magn. Resonance,* Vol 2, 1991, p 647
31. A.K. Gangopadhyay, P.A. Willermet, W.C. Vassell, and M.A. Tamor, *Tribol. Int.*, to be published
32. A.K. Gangopadhyay, P.A. Willermet, M.A. Tamor, and W.C. Vassell, Amorphous Hydrogenated Carbon Films for Tribological Applications, *Proc. 3rd Int. Conf. Applications of Diamond Films and Related Materials,* National Institute of Standards and Technology, 1995, p 703
33. H. Ronkainen, Comparative Tribological and Adhesion Studies of Some Titanium Based Ceramic Coatings, *Surf. Coat. Technol.*, Vol 43-44, 1990, p 888
34. S.J. Bull, D.S. Rickerby, and A. Jain, The Sliding Wear of Titanium Nitride Coatings, *Surf. Coat. Technol.*, Vol 41, 1990, p 269
35. T. Jamal, R. Nimmagadda, and R.P. Bunshah, Wear of Titanium Carbide and Nitride Coatings, *Thin Solid Films,* Vol 73, 1980, p 245
36. X. Jiang, W. Beyer, and K. Reichelt, Gas Evolution from Hydrogenated Amorphous Carbon Films, *J. Appl. Phys.*, Vol 68, 1990, p 1378
37. A. Grill, V. Patel, and B.S. Meyerson, Optical and Tribological Properties of Heat Treated Diamondlike Carbon, *J. Mater. Res.*, Vol 5 (No. 11), 1990, p 2531
38. M. Grischke, K. Bewilogua, K. Trojan, and H. Dimigen, Application Oriented Modification of Deposition Processes for Diamondlike Carbon-Based Coatings, *Surf. Coat. Technol.*, Vol 74-75, 1995, p 739
39. I.M. Hutchings, Cambridge University, private communication